

Attractor learning for spatiotemporally chaotic dynamical systems using echo state networks with transfer learning

Mohammad Shah Alam* William Ott† Ilya Timofeyev‡

June 13, 2025

Abstract

In this paper, we explore the predictive capabilities of echo state networks (ESNs) for the generalized Kuramoto-Sivashinsky (gKS) equation, an archetypal nonlinear PDE that exhibits spatiotemporal chaos. We introduce a novel methodology that integrates ESNs with transfer learning, aiming to enhance predictive performance across various parameter regimes of the gKS model. Our research focuses on predicting changes in long-term statistical patterns of the gKS model that result from varying the dispersion relation or the length of the spatial domain. We use transfer learning to adapt ESNs to different parameter settings and successfully capture changes in the underlying chaotic attractor.

Keywords: echo state networks, reservoir computing, generalized Kuramoto-Sivashinsky equation, transfer learning

1 Introduction

Over the past decade, there has been a substantial increase in research focused on the application of machine learning to dynamical systems. Neural networks have played a particularly important role, as a variety of promising techniques based on neural network architectures have been developed. In particular, reservoir computing [31, 58, 59] has been successfully utilized to learn and predict the dynamics of complex systems, including chaotic models. Reservoir computing refers to a broad class of recurrent neural networks, wherein the reservoir has its own nonlinear dynamics and only a linear output layer is trained to match the observational data.

In this paper, we explore the predictive capabilities of echo state networks (ESNs) in the context of spatiotemporal chaos. An echo state network is a simple reservoir computing architecture with the echo state property [7, 21, 28, 29, 30, 39, 58]. We introduce a novel methodology that integrates ESNs with transfer learning (TL). Our goal is to demonstrate that this novel methodology significantly enhances predictive performance when predicting changes in long-term statistical behavior that result from varying model parameters.

We describe our approach in the context of flows on metric spaces. Let (M, d) be a metric space and let $\Phi : M \times [0, \infty) \rightarrow M$ be a continuous map that defines a flow on M . That is, we have

*Dept. of Mathematics, Sul Ross University, msa24gn@sulross.edu

†Dept. of Mathematics, University of Houston, Houston, TX 77204, william.ott.math@gmail.com

‡Dept. of Mathematics, University of Houston, Houston, TX 77204, itimofey@Central.uh.edu

$\Phi^{t+s} = \Phi^t \circ \Phi^s$ for all $s, t \geq 0$, where $\Phi^t(\cdot) = \Phi(\cdot, t)$. Think of M as a function space and Φ as a flow on this function space generated by an evolution partial differential equation. Research at the interface of machine learning and dynamical systems has asked the following question. Can Φ be learned for predictive purposes?

The single-orbit approach asks the machine learning architecture to predict individual trajectories of Φ once training is complete. Echo state networks have been successfully used to predict trajectories of complex models, including chaotic systems [11, 14, 19, 22, 23, 25, 42, 46]. It is challenging, though, to prove rigorous mathematical lower bounds for the length of time the single-orbit predictions remain accurate. Alternatively, one can ask the machine learning architecture to learn and then predict statistical properties of the dynamics. This approach has also succeeded. Indeed, echo state networks can learn statistical properties of attractors of chaotic systems [3, 37, 38, 45, 46, 48, 51, 56].

In this paper, we focus on the following problem. Suppose that the flow Φ depends on a parameter γ . We write Φ_γ to indicate this dependence. For example, γ could be a parameter in the PDE that generates the flow Φ_γ . Suppose that for each γ in some parameter set Γ , the flow Φ_γ admits an attractor that supports an ergodic invariant measure μ_γ . Suppose further that for each $\gamma \in \Gamma$, μ_γ describes the asymptotic distribution of the orbit of a typical $x \in M$, meaning that

$$\lim_{T \rightarrow \infty} \frac{1}{T} \int_0^T \delta_{\Phi_\gamma^s(x)} = \mu_\gamma \quad (1)$$

in the weak-* topology. In this setting, we ask two questions. First, if we fix a parameter value $\gamma_1 \in \Gamma$ and train an echo state network using trajectories from Φ_{γ_1} , can the echo state network then predict statistical properties of $(f \circ \Phi_{\gamma_1}^t)_{t \geq 0}$, where $f : M \rightarrow \mathbb{R}^n$ is a given observable? Second, assuming an affirmative answer to the first question, how might we predict the statistical properties of $(f \circ \Phi_{\gamma_2}^t)_{t \geq 0}$ with respect to a *different* parameter value $\gamma_2 \in \Gamma$?

The point of this paper is to answer these two questions. Our approach is as follows. Suppose the echo state network has been trained using trajectories from Φ_{γ_1} and can successfully predict statistical properties of $(f \circ \Phi_{\gamma_1}^t)_{t \geq 0}$. Since invariant measures of dynamical systems can depend sensitively on parameters, the invariant measure μ_{γ_2} associated with a different parameter value γ_2 might differ meaningfully from μ_{γ_1} . Consequently, we would not expect the echo state network to successfully predict statistical properties of $(f \circ \Phi_{\gamma_2}^t)_{t \geq 0}$ when trained using trajectories from Φ_{γ_1} . We conjecture that the predictive capability of the echo state network can be ‘transferred’ from the γ_1 -system to the γ_2 -system using transfer learning [11, 27]. That is, the echo state network will successfully predict statistical properties of $(f \circ \Phi_{\gamma_2}^t)_{t \geq 0}$ after we update its training using a small new dataset from the new regime.

We show that our proposed approach succeeds for the generalized Kuramoto-Sivashinsky (gKS) equation, an archetypal nonlinear PDE that exhibits spatiotemporal chaos. We train an echo state network to accurately predict the statistics of gKS dynamics. We then show that transfer learning allows the echo state network to retain predictive power as we vary a parameter in the dispersion relation of the gKS equation or the length of the physical domain.

Transfer learning is a popular concept in many areas of machine learning, including speech recognition and image processing. However, transfer learning for echo state networks has received comparatively little attention in the literature. We conclude that transfer learning can allow echo state networks to maintain predictive power as model parameters change. Such flexibility is important when statistical properties of the dynamics depend meaningfully on model parameters.

2 KS and gKS equations

2.1 Background

The one-dimensional Kuramoto-Sivashinsky (KS) equation [36, 49] has become a canonical model for the study of spatiotemporal chaos. The one-dimensional KS equation is given by

$$\frac{\partial u}{\partial t} + \frac{\partial^2 u}{\partial x^2} + \frac{\partial^4 u}{\partial x^4} + u \frac{\partial u}{\partial x} = 0, \quad (2)$$

with the periodic boundary condition $u(x+L, t) = u(x, t)$ for all x and every $t \geq 0$. The KS equation is well-behaved as an infinite-dimensional dynamical system. In particular, the KS model admits a finite-dimensional attractor and is therefore in some sense equivalent to a finite-dimensional dynamical system [13, 20, 43]. See [52] for an overview. Moreover, the KS model admits an inertial manifold that contains the global attractor [12, 32, 53]. The KS equation has been studied extensively, both analytically and computationally [26, 35, 41, 50].

The parameter L (the length of the spatial domain) plays the role of a bifurcation parameter for the KS model. This parameter determines the number of linearly unstable Fourier modes, S_{unst} . In addition, the maximum of the coefficient of the linearized equation occurs at M_{unst} . We refer to M_{unst} as "the most unstable wavenumber". These quantities are given by

$$S_{\text{unst}} = \left\lfloor \frac{L}{2\pi} \right\rfloor, \quad M_{\text{unst}} = \frac{L}{2\sqrt{2}\pi}. \quad (3)$$

Here $\lfloor \cdot \rfloor$ denotes the greatest integer function.

The one-dimensional generalized Kuramoto-Sivashinsky equation is obtained from (2) by adding a parametric dispersion term (third derivative). The gKS equation is given by

$$\frac{\partial u}{\partial t} + \frac{\partial^2 u}{\partial x^2} + \gamma \frac{\partial^3 u}{\partial x^3} + \frac{\partial^4 u}{\partial x^4} + u \frac{\partial u}{\partial x} = 0, \quad (4)$$

where γ is a parameter. The boundary conditions are again periodic.

The dynamics of the gKS equation have been studied extensively [5, 8, 9, 15, 16, 18, 33, 34, 40, 47, 54, 55]. The parameter γ has a strong influence on gKS dynamics. For positive values of γ near zero, the gKS model exhibits spatiotemporal chaos, like the KS model does. As γ increases, the gKS model exhibits a transition toward less chaotic or even non-chaotic dynamics (see [24] for a detailed numerical study). In the limit $\gamma \rightarrow \infty$, the gKS equation is equivalent to the integrable Korteweg-de Vries (KdV) equation [55].

In this paper, we focus on statistical prediction as the parameters L and γ vary.

2.2 Numerical method

We use numerical solutions of the gKS equation to train ESNs. In this subsection, we describe the numerical method we use to integrate the gKS equation.

We use a uniform grid on $[0, L]$ and apply finite differences to discretize the derivatives in the gKS equation. In particular, we use an explicit method to discretize nonlinear fluxes and treat linear terms implicitly. We utilize Euler time-stepping. Therefore, the discrete version of the gKS equation reads

$$\frac{u_j^{n+1} - u_j^n}{\delta t} = -\frac{F_{j+1/2}^n - F_{j-1/2}^n}{\Delta x} + f(\mathbf{u}^{n+1}), \quad (5)$$

where $F_{j+1/2} = \frac{1}{6}((u_j^n)^2 + u_j^n u_{j+1}^n + (u_{j+1}^n)^2)$, $f(\mathbf{u}^{n+1})$ represents the discretization of the linear second, third, and fourth derivatives, and $\mathbf{u}^{n+1} = \{u_j^{n+1} : j = 1, \dots, N_x\}$ is the discrete solution vector at time $n + 1$. The second, third, and fourth derivatives are discretized using standard $O(\Delta x^2)$ central finite-difference formulas.

3 Echo state networks and transfer learning

Recurrent neural networks can be challenging to train. Reservoir computing has emerged as an elegant solution to the training challenge [28, 30, 39]. This is so because the reservoir has its own nonlinear dynamics and only a linear output layer is trained to match the observational data. Reservoir computers can successfully predict chaotic dynamics [6, 10, 31, 42, 45, 57]. They have been successfully applied in a variety of fields, including climate and weather prediction [4, 42], turbulent convection [44], and others [10, 57].

In this paper, we use the following standard ESN architecture. The ESN consists of an input layer, a reservoir of D neurons, and an output layer. Connections between the neurons are encoded by an adjacency matrix A . The reservoir processes successive inputs, where the reservoir state at time $t + \Delta t$, $r(t + \Delta t) \in \mathbb{R}^D$, is a nonlinear function of the previous reservoir state, $r(t) \in \mathbb{R}^D$, and the driving input, $X(t)$, given by

$$r(t + \Delta t) = f(Ar(t) + W_{\text{in}}X(t)). \quad (6)$$

Here $f = \tanh : \mathbb{R}^D \rightarrow \mathbb{R}^D$ is the element-wise activation function. Let N_x denote the dimension of the input. Matrices $A \in \mathbb{R}^{D \times D}$ and $W_{\text{in}} \in \mathbb{R}^{N_x \times D}$ remain constant throughout the training process. During training, only the weights of the output layer, $W_{\text{out}} \in \mathbb{R}^{D \times N_x}$, are tuned. Predictions are given by

$$X(t + \Delta t) = W_{\text{out}}\phi(r(t + \Delta t)), \quad (7)$$

where ϕ is the nonlinear transformation [10, 45] given component-wise by

$$\tilde{r}_j(t) = \phi(r_j(t)) = \begin{cases} r_j^2(t) & \text{if } j \text{ is even} \\ r_j(t) & \text{if } j \text{ is odd.} \end{cases} \quad (8)$$

We found in our experiments that this nonlinear transformation slightly improves the quality of predictions for individual trajectories.

The input matrix W_{in} is generated component-wise from a uniform distribution on $[-\beta_1, \beta_1]$. The adjacency matrix is generated as $A = \beta_2 W_0 / \lambda$, where W_0 is a sparse matrix (typically turning on less than 10% of the possible connections), λ denotes the largest eigenvalue of W_0 , and β_2 is a scaling parameter.

The weights of $W_{\text{out}} \in \mathbb{R}^{D \times N_x}$ are determined through a linear regression with L^2 -regularization by

$$W_{\text{out}} = \arg \min_W \|WR - \mathbf{X}\|_2^2 + \mu \|W\|_2^2, \quad (9)$$

where \mathbf{X} is the training data (trajectories), and \mathbf{R} denotes the reservoir timeseries (with A and W_{in} fixed). W_{out} can be expressed explicitly as

$$W_{\text{out}} = \mathbf{X}\mathbf{R}'(\mathbf{R}\mathbf{R}' + \mu I)^{-1}. \quad (10)$$

Here, \mathbf{R}' denotes the transpose of \mathbf{R} . Throughout this paper, we use ESN parameters $D = 5000$, $\beta_1 = 0.01$, $\beta_2 = 0.1$, and $\mu = 0.000005$, unless stated otherwise.

Transfer learning [11, 27] is a machine-learning approach wherein knowledge in a source domain is used to improve predictive performance in a target domain. In our context, the source and target domains are simply two sets of gKS parameters. Our central premise for linking transfer learning to ESNs is the following. Once the ESN is well trained in the source domain, it will retain predictive power in the target domain after receiving a training update using a small transfer-learning dataset from the target domain.

Writing \mathbf{X}_{TL} for the transfer-learning dataset, the update to the output layer is obtained by solving the optimization problem given by

$$\delta W = \arg \min_{\delta W} \|(W_{\text{out}} + \delta W)\mathbf{R}_{TL} - \mathbf{X}_{TL}\|_2^2 + \alpha \|\delta W\|_2^2. \quad (11)$$

Here, α is the rate of transfer learning and \mathbf{R}_{TL} is the (time-dependent) state of the reservoir (with the same number of time-snapshots as \mathbf{X}_{TL}). The update to the output layer and new output layer are given explicitly by

$$\begin{aligned} \delta W &= (\mathbf{X}_{TL}\mathbf{R}'_{TL} - W_{\text{out}}\mathbf{R}_{TL}\mathbf{R}'_{TL})(\mathbf{R}_{TL}\mathbf{R}'_{TL} + \alpha I)^{-1}, \\ W_{\text{out}}^{\text{new}} &= W_{\text{out}} + \delta W. \end{aligned} \quad (12)$$

Here, W_{out} and $W_{\text{out}}^{\text{new}}$ are the output layer in the source and target domains, respectively.

Transfer learning has been used with ESNs to successfully predict individual trajectories for shallow-water equations [1, 11] and the gKS equation [1]. In this paper, we show that transfer learning allows us to successfully track changes in the statistical signature of the gKS equation as either the size of the spatial domain or the dispersion relation vary.

4 Results

We focus on an important statistical feature of gKS dynamics, namely the power spectrum. The power spectrum is defined as the map from \mathbb{Z} into \mathbb{R} given by

$$k \mapsto e_k = \frac{1}{T} \int_0^T |\hat{u}_k(t)|^2 dt, \quad (13)$$

where $\hat{u}_k(t)$ is coefficient k at time t of the Fourier-series representation of the solution to the gKS equation,

$$u(x, t) = \sum_{k \in \mathbb{Z}} \hat{u}_k(t) e^{(2\pi i k/L)x}. \quad (14)$$

The quantity e_k represents the average energy in Fourier wavenumber k . Since the solution $u(x, t)$ of the gKS equation is real-valued, the Fourier coefficients satisfy $\hat{u}_{-k} = \hat{u}_k^*$. We therefore consider only nonnegative wavenumbers.

Throughout Section 4, we work with the gKS equation in the chaotic regime ($\gamma = 0$ or γ is small and positive). We assume the gKS equation admits an attractor that supports an ergodic measure. We assume that this ergodic measure describes the distribution of the orbit of the initial data we

select. (As γ increases, the gKS equation eventually becomes less chaotic [24]. In particular, the power spectrum depends on the initial data when γ is sufficiently large.)

We first consider the KS equation and we vary the parameter L . Varying L is equivalent to varying the number of linearly unstable Fourier modes. We show that for each of several values of L , the ESN accurately predicts the power spectrum of the KS equation with spatial domain $[0, L]$, once trained using KS trajectories from the same spatial domain. We then show that transfer learning is effective for various tuples (L_1, L_2) of length parameters. That is, the ESN accurately predicts the power spectrum of the KS equation with parameter L_2 after a two-step training process. First, the ESN is trained using trajectories of the KS equation with parameter L_1 . Second, the training is updated using a small amount of trajectory information from the KS equation with parameter L_2 .

We conclude Section 4 by carrying out the program in the previous paragraph for the gKS equation. This time, we fix L and vary the parameter γ in the dispersion relation. We show that when γ is small, the ESN accurately predicts power spectra and transfer learning is effective.

4.1 Resolution study

In [1, Section 5.1.3], Alam analyzed numerically how spatial resolution affects the performance of ESNs when using them to predict the power spectrum of the gKS equation. In particular, Alam considered $L = 43$ and $\gamma = 0.1$ and analyzed how numerically computed power spectra depend on the spatial resolution. In addition, Alam investigated how averaging time affects the accuracy of the computation of power spectra. Alam determined that spatial resolution $N_x = 256$, averaging time $T = 1000$ Lyapunov times, integration timestep $\delta t = 0.001$, and snapshot sampling timestep $\Delta t = 0.25$ are sufficient to accurately reproduce the power spectrum of the gKS equation in the chaotic regime. We therefore use these parameter values for the simulations in this paper, unless stated otherwise.

4.2 Predicting the power spectrum of the KS equation

4.2.1 Predicting the power spectrum of the KS equation without transfer learning

We show that for each of several values of L , the ESN accurately predicts the power spectrum of the KS equation with spatial domain $[0, L]$, once trained using KS trajectories from the same spatial domain. We consider four values of L that correspond to four different numbers of linearly unstable Fourier modes. Table 1 lists each choice of L , together with the corresponding number of linearly unstable Fourier modes (S_{unst}), the most unstable wavenumber (M_{unst}), and an approximation of λ_{max} , the maximal Lyapunov exponent. We use the approximation for the Lyapunov exponents ($\lambda_0 \geq \lambda_1 \geq \dots \geq \lambda_i \geq \dots$) given in [17] by

$$\lambda_i(L) \approx 0.093 - 0.94(i - 0.39)/L. \quad (15)$$

We performed the following experiment for each value of L . We began with an untrained ESN. We generated 30 KS trajectories of length $T = 1000$ Lyapunov times using random initial data of the form

$$u(x, 0) = c_1 \cos\left(\frac{p_1 x \pi}{L}\right) + c_2 \cos\left(\frac{p_2 x \pi}{L}\right), \quad (16)$$

where we independently selected $c_1, c_2 \sim \text{Uniform}([0, 1])$ and $p_1, p_2 \sim \text{Uniform}(\{1, 2, 3, 4, 5, 6\})$. We used 20 of these trajectories to train the ESN and the other 10 for prediction.

Table 1: Values of L for which we predict the power spectrum of the KS equation with spatial domain $[0, L]$. For each value of L , we list the number of linearly unstable Fourier modes (S_{unst}) given by (3), the most unstable wavenumber (M_{unst}) given by (3), and an approximation of the maximal Lyapunov exponent (given in [17] and by (15)).

L	S_{unst}	M_{unst}	λ_{max}
22	3	2.48	0.1097
29	4	3.26	0.1056
35	5	3.94	0.1035
43	6	4.84	0.1015

Before considering prediction of the power spectrum, it is natural to ask how well the trained ESN predicts individual KS trajectories. Alam [1, Section 4.3.2] investigated this question. He found that ESN predictions of individual trajectories remain accurate up to approximately 7 Lyapunov times. This timescale is consistent with results published earlier [45]. Alam [1, Section 4.3.2] found that the timescale for which predictions of individual trajectories remains accurate decays approximately linearly with L . As L increases, one can potentially deal with this decay by training a larger ESN or by training a coupled network of ESNs. Nevertheless, we are unaware of rigorous mathematical guarantees associated with single-orbit prediction of spatiotemporally chaotic dynamics using ESNs. That is, we are unaware of rigorous lower bounds on the number of Lyapunov times for which the single-orbit prediction remains accurate. This motivates our focus on the power spectrum. The idea is that once the ESN can predict the power spectrum, it can do so for a very long time. In particular, it can continue to accurately predict the power spectrum long after single-orbit predictions have become inaccurate.

Figure 1 demonstrates that for each of the four values of L in Table 1, the ESN accurately predicts the power spectrum of the KS equation (once trained). Each panel compares the power spectrum obtained by direct numerical simulation (DNS) to the ESN prediction. We average over 10 trajectories used for prediction to obtain each DNS-based curve.

4.2.2 Predicting the power spectrum of the KS equation using transfer learning

When L varies, it is computationally expensive to train a *de novo* ESN to predict the power spectrum for each new value of L . We therefore investigate the efficacy of transfer learning with respect to L for the prediction of the power spectrum.

We consider $L = 22$ and $L = 43$, values of L that correspond to the presence of 3 and 6 linearly unstable Fourier modes, respectively. Importantly, the power spectrum for $L = 43$ differs considerably from the power spectrum for $L = 22$ (Figure 2, blue and red curves, respectively).

We performed the following experiment. First, we trained the ESN in the $L = 22$ regime using 20 trajectories from that regime. Second, we set the transfer learning rate to $\alpha = 0.005$ and then updated the training of the ESN using trajectory data from the $L = 43$ regime. (We tested several values of α , including 0.1, 0.01, 0.005, 0.002, and 0.001. Empirically, $\alpha = 0.005$ worked well.) We report the amount of TL data used for the training update as a percentage of the 20 trajectories from the $L = 43$ regime used for training.

In the absence of transfer learning, the ESN (trained only on trajectories from the $L = 22$ regime) performs poorly in the $L = 43$ regime for both single-orbit prediction and the prediction of the power spectrum [1]. However, transfer learning dramatically improves the prediction of the

power spectrum in the $L = 43$ regime. Figure 2 illustrates this dramatic improvement as a function of amount of TL data. The blue curve (same curve in each panel) is the power spectrum in the $L = 43$ regime, computed by averaging over the 10 DNS trajectories from this regime used for prediction. This curve serves as ground truth. The red curve (same curve in each panel) is the power spectrum for $L = 22$ predicted by the ESN after having been trained on 20 DNS trajectories from the $L = 22$ regime. Comparing the red and blue curves, we see that the power spectrum for $L = 22$ differs considerably from that for $L = 43$. The green curves illustrate the ESN prediction of the power spectrum for the $L = 43$ regime after transfer learning of level 10% (left), 25% (center), and 50% (right). The quality of the prediction based on transfer learning rapidly improves as the level of TL data increases. In particular, the prediction is nearly perfect at level 50% (right).

4.3 Predicting the power spectrum of the gKS equation

We consider the gKS equation when the parameter γ in the dispersion relation is small. We assume that for γ small, the gKS dynamics admit an attractor that supports an ergodic invariant measure. We assume that this invariant measure describes the asymptotic distribution of all of the initial data that we select. We show that for γ small and fixed, the ESN accurately predicts the power spectrum of the gKS equation for this fixed value of γ , once trained on trajectories generated using this fixed value of γ . We then show that transfer learning is remarkably effective for small γ . Throughout Section 4.3, we set $L = 43$.

4.3.1 Predicting the power spectrum of the gKS equation without transfer learning

We performed the following experiment for each of two values of γ , $\gamma = 0$ and $\gamma = 0.1$. We began with an untrained ESN. We generated 30 gKS trajectories, each of length $T = 1000$ Lyapunov times, via direct numerical simulation. We used 20 of these to train the ESN and the other 10 for prediction.

Figure 3 illustrates that for $\gamma = 0$ (left) and $\gamma = 0.1$ (right), the trained ESN accurately predicts the power spectrum of the gKS equation. Each red curve shows the ESN prediction of the power spectrum. Each blue curve shows the power spectrum obtained by averaging over the 10 trajectories used for prediction. Importantly, the power spectrum of the gKS equation depends sensitively on γ in the chaotic (small γ) regime. This observation serves as serious motivation for the use of transfer learning in this regime.

4.3.2 Predicting the power spectrum of the gKS equation with transfer learning

Figure 3 demonstrates that the statistical behavior of the gKS equation depends sensitively on γ in the small- γ regime. We therefore ask if transfer learning can capture substantial changes in statistical behavior as γ varies. To address this question, we performed the following experiment. We started with an untrained ESN and first trained it using 20 trajectories from the $\gamma = 0$ regime. We then updated the training using a small amount of TL data from the $\gamma = 0.1$ regime at transfer learning rate $\alpha = 0.005$.

The result of this experiment is shown in Figure 4 (left). The blue curve shows the ground truth, namely the power spectrum in the $\gamma = 0.1$ regime obtained by averaging over the 10 trajectories from the $\gamma = 0.1$ regime used for prediction. Using a transfer learning level of only 10% (2 trajectories) produces an accurate ESN prediction of the power spectrum (green curve). For reference, the yellow curve shows the ESN-based prediction of the power spectrum when the ESN is trained only on 20

trajectories from the $\gamma = 0$ regime. Importantly, the accurate TL-based prediction of the power spectrum is valid over long timescales. By contrast, single-orbit predictions in the $\gamma = 0.1$ regime based on transfer learning are valid for shorter timescales [1, Section 5.1.1].

As a control, we compare the prediction using transfer learning (Figure 4, green curve, ESN-TL) to a prediction from an ESN that has been trained only on the TL data, namely 2 trajectories from the $\gamma = 0.1$ regime (Figure 4, red curve, ESN*). We see that the ESN* prediction is inferior to the ESN-TL prediction in the eye metric. Discrepancies between these two predictions occur at low wavenumbers that contain most of the energy. Quantitatively, the curves shown in Figure 4 (right) contain total energies 2.92 (blue, DNS), 2.80 (red, ESN*), and 2.97 (green, ESN-TL). This corresponds to relative error 4.1% and 1.7% for the ESN* and ESN-TL predictions, respectively. In the relative-error metric, the ESN-TL prediction is more than twice as accurate as the ESN* control.

5 Discussion

The interface of machine learning and dynamical systems is a rapidly developing field. Echo state networks have emerged as a powerful tool. For spatiotemporally chaotic systems, these networks are capable of both single-orbit and statistical prediction. In this paper, we have focused on predicting the long-term statistical behavior of an archetypal model, the gKS equation in the spatiotemporally chaotic regime.

We have shown that when the domain size L and the dispersion parameter γ are fixed, our ESN can learn and then accurately predict the power spectrum of the gKS equation. Further, we have shown that transfer learning allows one to efficiently and accurately track changes in the power spectrum of the gKS equation as L or γ varies. Importantly, our ESN did not blow up nor collapse during our long simulations. This is a great sign for the utility of ESNs with respect to long-term statistical prediction.

Looking to the future, ESNs can potentially be used as an inexpensive climate simulator or a chaotic heat bath. Importantly, ESNs allow relatively large timesteps when generating new trajectories, making them more efficient than traditional numerical integrators. Thus far, transfer learning for ESNs has received limited attention in the literature. We believe transfer learning is an important concept that can be applied to complex problems and allow ESNs to track parametric changes in spatiotemporally chaotic dynamics. In general, developing efficient models that can track parametric changes in dynamical systems is an important task. The methodology described in this paper aims at this goal.

6 Code

Our code for simulating the gKS equation and ESNs is located on GitHub [2].

7 Author contributions

All authors wrote the paper. Study design: WO, IT. Initial code development: IT. Code development, simulation, and visualization: MSA.

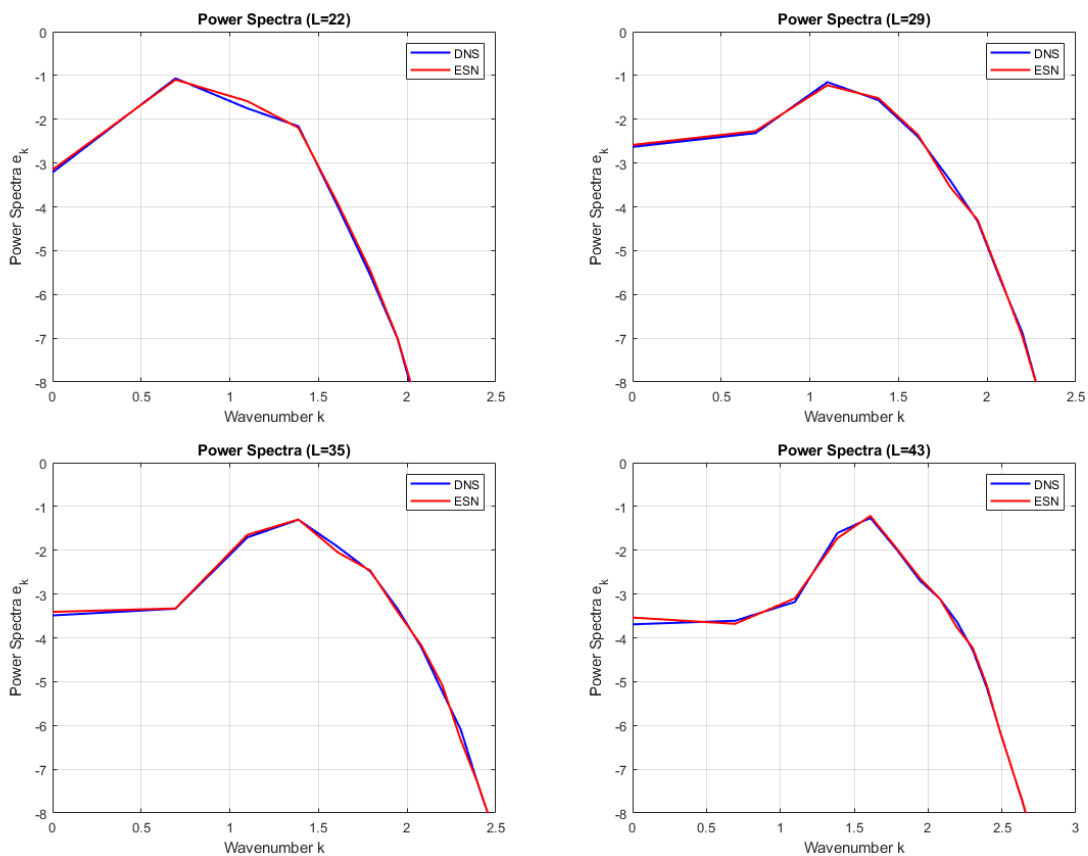


Figure 1: Once trained on KS trajectories from spatial domain $[0, L]$, the ESN then accurately predicts the power spectrum of the KS equation with the same spatial domain. Each blue curve shows the power spectrum obtained from direct numerical simulation, averaged over 10 trajectories used for prediction. Red curves show the ESN predictions of the power spectrum. Importantly, the ESN predictions of the power spectrum remain accurate long after ESN predictions of individual trajectories become inaccurate. Spatial domain sizes $L = 22$ (top left), $L = 29$ (top right), $L = 35$ (bottom left), and $L = 43$ (bottom right) correspond to four different numbers of linearly unstable Fourier modes (see Table 1). Plots show $\log(e_k)$ versus $\log(k)$, where k denotes wavenumber.

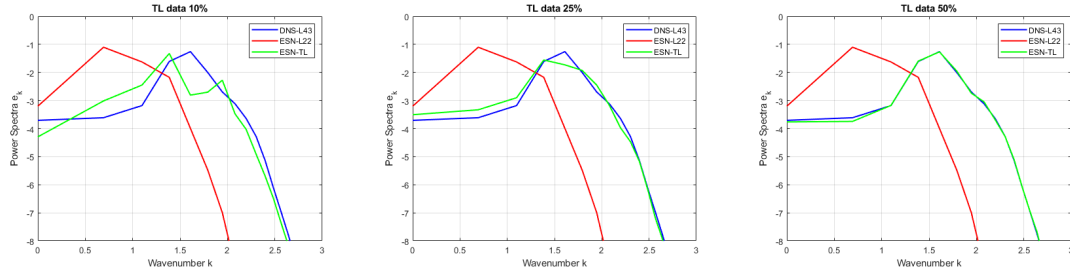


Figure 2: Transfer learning allows the ESN to accurately predict the power spectrum of the KS equation as the size of the spatial domain varies. Curves illustrate power spectra. DNS-L43: Power spectrum obtained by averaging over the 10 trajectories in the $L = 43$ regime used for prediction. ESN-L22: Power spectrum for the $L = 22$ regime predicted by the ESN, once it is trained on 20 trajectories from the $L = 22$ regime. ESN-TL: Power spectrum for the $L = 43$ regime predicted by the ESN after transfer learning of level 10% (left), 25% (middle), and 50% (right). Plots show $\log(e_k)$ versus $\log(k)$, where k denotes wavenumber.

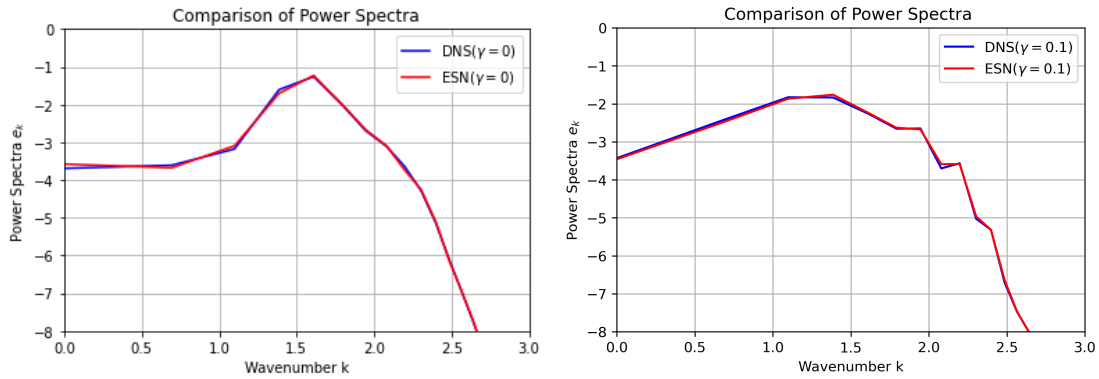


Figure 3: Once trained, the ESN accurately predicts the power spectrum of the gKS equation. Left: $\gamma = 0$. Right: $\gamma = 0.1$. Each blue curve shows the power spectrum obtained by averaging over the 10 DNS trajectories used for prediction. Each red curve shows the power spectrum predicted by the ESN, after the untrained ESN has been trained using 20 trajectories. Plots show $\log(e_k)$ versus $\log(k)$, where k denotes wavenumber.

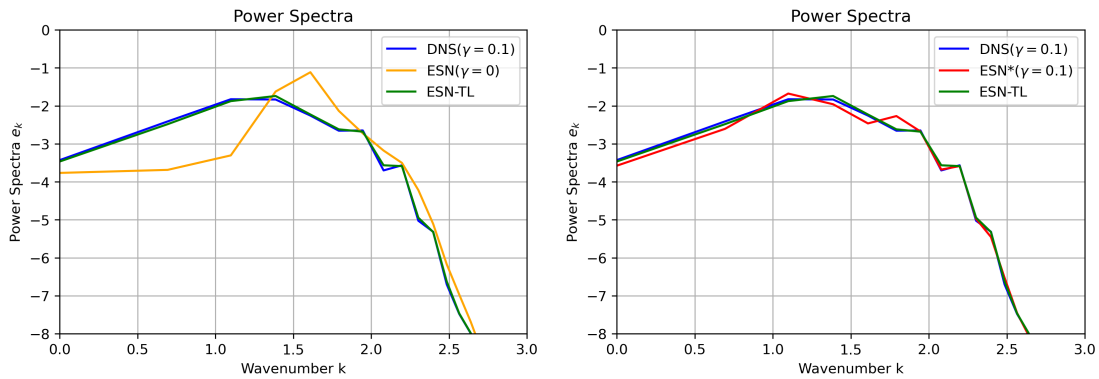


Figure 4: Transfer learning allows the ESN to accurately predict the power spectrum of the gKS equation as the dispersion parameter γ varies. Blue curve (same curve in both panels): Power spectrum of the gKS equation in the $\gamma = 0.1$ regime obtained by averaging over the 10 DNS trajectories used for prediction. Green curve (same curve in both panels): Power spectrum predicted by the ESN after a first round of training using 20 trajectories from the $\gamma = 0$ regime and then a training update using TL data from the $\gamma = 0.1$ regime at level 10%. Yellow curve: Power spectrum predicted by the ESN after training only on 20 trajectories from the $\gamma = 0$ regime. Red curve: Power spectrum predicted by an ESN that has been trained only on the TL data, namely 2 trajectories from the $\gamma = 0.1$ regime. Plots show $\log(e_k)$ versus $\log(k)$, where k denotes wavenumber.

References

- [1] M. S. ALAM, *Data-Driven Predictions of Dynamical Systems using Echo State Network with Transfer Learning*, PhD thesis, University of Houston, 2024.
- [2] ———, *Attractor learning for spatiotemporally chaotic dynamical systems using echo-state networks with transfer learning*. <https://github.com/shahalam1005/ESNgKS/tree/main>, 2025. GitHub repository.
- [3] P. ANTONIK, M. GULINA, J. PAUWELS, AND S. MASSAR, *Using a reservoir computer to learn chaotic attractors, with applications to chaos synchronization and cryptography*, *Physical Review E*, 98 (2018), p. 012215.
- [4] T. ARCOMANO, I. SZUNYOGH, J. PATHAK, A. WIKNER, B. R. HUNT, AND E. OTT, *A machine learning-based global atmospheric forecast model*, *Geophysical Research Letters*, 47 (2020), p. e2020GL087776.
- [5] N. BALMFORTH, *Solitary waves and homoclinic orbits*, *Annual review of fluid mechanics*, 27 (1995), pp. 335–373.
- [6] E. BOLLT, *On explaining the surprising success of reservoir computing forecaster of chaos? the universal machine learning dynamical system with contrast to var and dmd*, *Chaos: An Interdisciplinary Journal of Nonlinear Science*, 31 (2021).
- [7] M. BUEHNER AND P. YOUNG, *A tighter bound for the echo state property*, *IEEE Transactions on Neural Networks*, 17 (2006), pp. 820–824.
- [8] H.-C. CHANG, E. DEMEKHIN, AND E. KAL Aidin, *Interaction dynamics of solitary waves on a falling film*, *Journal of Fluid Mechanics*, 294 (1995), pp. 123–154.
- [9] H.-C. CHANG, E. A. DEMEKHIN, AND D. I. KOPELEVICH, *Laminarizing effects of dispersion in an active-dissipative nonlinear medium*, *Physica D: Nonlinear Phenomena*, 63 (1993), pp. 299–320.
- [10] A. CHATTOPADHYAY, P. HASSANZADEH, AND D. SUBRAMANIAN, *Data-driven predictions of a multiscale Lorenz 96 chaotic system using machine-learning methods: reservoir computing, artificial neural network, and long short-term memory network*, *Nonlinear Processes in Geophysics*, 27 (2020), pp. 373–389.
- [11] X. CHEN, B. T. NADIGA, AND I. TIMOFEYEV, *Predicting shallow water dynamics using echo-state networks with transfer learning*, *GEM-International Journal on Geomathematics*, 13 (2022), p. 20.
- [12] P. COLLET, J.-P. ECKMANN, H. EPSTEIN, AND J. STUBBE, *Analyticity for the Kuramoto-Sivashinsky equation*, *Physica D: Nonlinear Phenomena*, 67 (1993), pp. 321–326.
- [13] P. CONSTANTIN, C. FOIAS, B. NICOLAENKO, AND R. TEMAM, *Integral manifolds and inertial manifolds for dissipative partial differential equations*, vol. 70, Springer Science & Business Media, 2012.

- [14] N. A. K. DOAN, W. POLIFKE, AND L. MAGRI, *Physics-informed echo state networks*, Journal of Computational Science, 47 (2020), p. 101237.
- [15] C. DUPRAT, F. GIORGIUTTI-DAUPHINÉ, D. TSELUIKO, S. SAPRYKIN, AND S. KALLIADASIS, *Liquid film coating a fiber as a model system for the formation of bound states in active dispersive-dissipative nonlinear media*, Physical review letters, 103 (2009), p. 234501.
- [16] C. DUPRAT, D. TSELUIKO, S. SAPRYKIN, S. KALLIADASIS, AND F. GIORGIUTTI-DAUPHINÉ, *Wave interactions on a viscous film coating a vertical fibre: Formation of bound states*, Chemical Engineering and Processing: Process Intensification, 50 (2011), pp. 519–524.
- [17] R. A. EDSON, J. E. BUNDER, T. W. MATTNER, AND A. J. ROBERTS, *Lyapunov exponents of the kuramoto–sivashinsky pde*, The ANZIAM Journal, 61 (2019), pp. 270–285.
- [18] S.-I. EI AND T. OHTA, *Equation of motion for interacting pulses*, Physical Review E, 50 (1994), p. 4672.
- [19] D. ESTÉVEZ-MOYA, E. ESTÉVEZ-RAMS, AND H. KANTZ, *Echo state networks for the prediction of chaotic systems*, in International Workshop on Artificial Intelligence and Pattern Recognition, Springer, 2023, pp. 119–128.
- [20] C. FOIAS, B. NICOLAENKO, G. SELL, AND R. TEMAM, *Inertial manifolds for the kuramoto–sivashinsky equation and an estimate of their lowest dimension*, Journal de Mathématiques Pures et Appliquées, 67 (1988), pp. 197–226.
- [21] M. GANDHI AND H. JAEGER, *Echo state property linked to an input: Exploring a fundamental characteristic of recurrent neural networks*, Neural Computation, 25 (2013), pp. 671–696.
- [22] M. GIRVAN, E. OTT, AND B. R. HUNT, *Separation of chaotic signals by reservoir computing*, Chaos: An Interdisciplinary Journal of Nonlinear Science, 30 (2020), p. 023123.
- [23] A. M. GONZÁLEZ-ZAPATA, E. TLELO-CUAUTLE, B. OVILLA-MARTINEZ, I. CRUZ-VEGA, AND L. G. DE LA FRAGA, *Optimizing echo state networks for enhancing large prediction horizons of chaotic time series*, Mathematics, 10 (2022), p. 3886.
- [24] H. GOTODA, M. PRADAS, AND S. KALLIADASIS, *Nonlinear forecasting of the generalized Kuramoto–Sivashinsky equation*, International Journal of Bifurcation and Chaos, 25 (2015), p. 1530015.
- [25] F. HEYDER AND J. SCHUMACHER, *Echo state network for two-dimensional turbulent moist rayleigh–bénard convection*, Phys. Rev. E, 103 (2021), p. 053107.
- [26] J. M. HYMAN, B. NICOLAENKO, AND S. ZALESKI, *Order and complexity in the kuramoto–sivashinsky model of weakly turbulent interfaces*, Physica D: Nonlinear Phenomena, 23 (1986), pp. 265–292.
- [27] M. INUBUSHI AND S. GOTO, *Transfer learning for nonlinear dynamics and its application to fluid turbulence*, Physical Review E, 102 (2020), p. 043301.
- [28] H. JAEGER, *The “echo state” approach to analysing and training recurrent neural networks—with an erratum note*, Bonn, Germany: German National Research Center for Information Technology GMD Technical Report, 148 (2001), p. 13.

- [29] ———, *Adaptive nonlinear system identification with echo state networks*, in Advances in Neural Information Processing Systems, S. Becker, S. Thrun, and K. Obermayer, eds., vol. 15, MIT Press, 2002.
- [30] ———, *Echo state network*, scholarpedia, 2 (2007), p. 2330.
- [31] H. JAEGER AND H. HAAS, *Harnessing nonlinearity: Predicting chaotic systems and saving energy in wireless communication*, Science, 304 (2004), pp. 78–80.
- [32] M. S. JOLLY, I. KEVREKIDIS, AND E. S. TITI, *Approximate inertial manifolds for the kuramoto-sivashinsky equation: analysis and computations*, Physica D: Nonlinear Phenomena, 44 (1990), pp. 38–60.
- [33] S. KALLIADASIS, C. RUYER-QUIL, B. SCHEID, AND M. G. VELARDE, *Falling liquid films*, vol. 176, Springer Science & Business Media, 2011.
- [34] T. KAWAHARA, *Formation of saturated solitons in a nonlinear dispersive system with instability and dissipation*, Physical review letters, 51 (1983), p. 381.
- [35] I. G. KEVREKIDIS, B. NICOLAENKO, AND J. C. SCOVEL, *Back in the saddle again: a computer assisted study of the kuramoto-sivashinsky equation*, SIAM Journal on Applied Mathematics, 50 (1990), pp. 760–790.
- [36] Y. KURAMOTO AND T. TSUZUKI, *Persistent propagation of concentration waves in dissipative media far from thermal equilibrium*, Progress of theoretical physics, 55 (1976), pp. 356–369.
- [37] Y. LI AND Y. LI, *Predicting chaotic time series and replicating chaotic attractors based on two novel echo state network models*, Neurocomputing, 491 (2022), pp. 321–332.
- [38] Z. LU, B. R. HUNT, AND E. OTT, *Attractor reconstruction by machine learning*, Chaos: An Interdisciplinary Journal of Nonlinear Science, 28 (2018), p. 061104.
- [39] W. MAASS, T. NATSCHLÄGER, AND H. MARKRAM, *Real-time computing without stable states: A new framework for neural computation based on perturbations*, Neural Computation, 14 (2002), pp. 2531–2560.
- [40] P. MANNEVILLE, *Liapounov exponents for the kuramoto-sivashinsky model*, in Macroscopic Modelling of Turbulent Flows: Proceedings of a Workshop Held at INRIA, Sophia-Antipolis, France, December 10–14, 1984, Springer, 1985, pp. 319–326.
- [41] M. MÜNDEL AND F. KAISER, *An intermittency route to chaos via attractor merging in the laser-kuramoto-sivashinsky equation*, Physica D: Nonlinear Phenomena, 98 (1996), pp. 156–170.
- [42] B. NADIGA, *Reservoir computing as a tool for climate predictability studies*, Journal of Advances in Modeling Earth Systems, (2021), p. e2020MS002290.
- [43] B. NICOLAENKO, B. SCHEURER, AND R. TEMAM, *Some global dynamical properties of the kuramoto-sivashinsky equations: nonlinear stability and attractors*, Physica D: Nonlinear Phenomena, 16 (1985), pp. 155–183.
- [44] S. PANDEY AND J. SCHUMACHER, *Reservoir computing model of two-dimensional turbulent convection*, Physical Review Fluids, 5 (2020), p. 113506.

- [45] J. PATHAK, B. HUNT, M. GIRVAN, Z. LU, AND E. OTT, *Model-free prediction of large spatiotemporally chaotic systems from data: A reservoir computing approach*, Physical Review Letters, 120 (2018), p. 024102.
- [46] J. PATHAK, Z. LU, B. R. HUNT, M. GIRVAN, AND E. OTT, *Using machine learning to replicate chaotic attractors and calculate lyapunov exponents from data*, Chaos: An Interdisciplinary Journal of Nonlinear Science, 27 (2017).
- [47] M. PRADAS, D. TSELUIKO, AND S. KALLIADASIS, *Rigorous coherent-structure theory for falling liquid films: Viscous dispersion effects on bound-state formation and self-organization*, Physics of Fluids, 23 (2011).
- [48] A. RACCA AND L. MAGRI, *Robust optimization and validation of echo state networks for learning chaotic dynamics*, Neural Networks, 142 (2021), pp. 252–268.
- [49] G. SIVASHINSKY, *Nonlinear analysis of hydrodynamic instability in laminar flames—i. derivation of basic equations*, Acta Astronautica, 4 (1977), pp. 1177–1206.
- [50] Y. S. SMYRLIS AND D. T. PAPAGEORGIOU, *Predicting chaos for infinite dimensional dynamical systems: the kuramoto-sivashinsky equation, a case study.*, Proceedings of the National Academy of Sciences, 88 (1991), pp. 11129–11132.
- [51] G. TANAKA, T. YAMANE, J. B. HÉROUX, R. NAKANE, N. KANAZAWA, S. TAKEDA, H. NUMATA, D. NAKANO, AND A. HIROSE, *Recent advances in physical reservoir computing: A review*, Neural Networks, 115 (2019), pp. 100–123.
- [52] R. TEMAM, *Infinite-dimensional dynamical systems in mechanics and physics*, vol. 68, Springer Science & Business Media, 2012.
- [53] R. TEMAM AND X. M. WANG, *Estimates on the lowest dimension of inertial manifolds for the Kuramoto-Sivashinsky equation in the general case*, Differential Integral Equations, 7 (1994), pp. 1095–1108.
- [54] D. TSELUIKO AND S. KALLIADASIS, *Weak interaction of solitary pulses in active dispersive-dissipative nonlinear media*, The IMA Journal of Applied Mathematics, 79 (2014), pp. 274–299.
- [55] D. TSELUIKO, S. SAPRYKIN, AND S. KALLIADASIS, *Interaction of solitary pulses in active dispersive-dissipative media*, Proceedings of the Estonian Academy of Sciences, 59 (2010), p. 139.
- [56] P. VLACHAS, J. PATHAK, B. HUNT, T. SAPSIS, M. GIRVAN, E. OTT, AND P. KOUMOUTSAKOS, *Backpropagation algorithms and reservoir computing in recurrent neural networks for the forecasting of complex spatiotemporal dynamics*, Neural Networks, 126 (2020), pp. 191–217.
- [57] P. R. VLACHAS, J. PATHAK, B. R. HUNT, T. P. SAPSIS, M. GIRVAN, E. OTT, AND P. KOUMOUTSAKOS, *Backpropagation algorithms and reservoir computing in recurrent neural networks for the forecasting of complex spatiotemporal dynamics*, Neural Networks, 126 (2020), pp. 191–217.
- [58] I. B. YILDIZ, H. JAEGER, AND S. J. KIEBEL, *Re-visiting the echo state property*, Neural Networks, 35 (2012), pp. 1–9.

- [59] H. ZHANG AND D. V. VARGAS, *A survey on reservoir computing and its interdisciplinary applications beyond traditional machine learning*, *IEEE Access*, 11 (2023), pp. 81033–81070.